Necrosis-associated long noncoding RNA for predicting prognosis in hepatocellular carcinoma

Xin Wang
Beijing YouAn Hospital, Capital Medical University
Jun Yang
Beijing YouAn Hospital, Capital Medical University
Zhenglai Ma
Beijing YouAn Hospital, Capital Medical University
Zhongjie Hu (huzhongjie@ccmu.edu.cn)
Beijing YouAn Hospital, Capital Medical University

Article

Keywords: necroptosis-related genes, hepatocellular carcinoma, prognosis, immune microenvironment, PD-L1

Posted Date: May 4th, 2023

DOI: https://doi.org/10.21203/rs.3.rs-2676108/v1

Abstract

Background and aim Histiocellular carcinoma (HCC) ranks second in the world's most deadly diseases, with a high mortality rate. Unlike apoptosis, necroptosis causes the release of molecular factors that elicit an immune response. As of yet, it has not been fully investigated how necroptotic machinery interacts with tumor-infiltrating lymphocytes in HCC .

Methods 374 patients and 50 healthy controls were analyzed using TCGA gene expression profiles, long noncoding RNA data and clinical characteristics. By analyzing lncRNA-seq data from 374 patients with HCC, an investigation of the relationships between necroptosis-related genes and tumor-infiltrating cells was conducted. A two-step multivariate Cox model and an univariate Cox model were analyzed to predict the prognosis . Nomograms were generated by combining necroptosis-related gene signatures with clinical characteristics. An analysis of HCC for PD-L1 was examined along with tumor-infiltrating immune cells .

Results Necroptosis-related pathways were enriched in lncRNA expression profiles in HCC tissues. The gene signature associated with necroptosis significantly reduced the survival rate of high-risk patients . The necroptosis-related gene signature demonstrated a high degree of predictive ability for OS (AUC= 0.781). Low-risk subgroups had significantly fewer aDCs, macrophages, and Treg cells than high-risk subgroups. In addition, scores indicating risk were positively correlated with uncharacterized cells, cancer associated fibroblast, monocyte, Macrophage/Monocyte and T cell regulatory (Tregs).

Conclusions These results revealed that the immunogenetic role of necroptosis may be influential in HCC prognosis. Exploring new possibilities for diagnostics and immunotherapy, the immune environment which was associated with necroptotic signatures needs to be assessed further based on its specific composition and functional characteristics.

INTRODUCTION

Hepatocellular carcinoma (HCC) is a type of liver cancer that originates from liver cells[1]. According to statistics, hepatocellular carcinoma is the second leading cause of cancer-related death in humans. Cirrhotic liver is responsible for approximately 80% of HCCs, which are caused by chronic viral infection, alcohol abuse, aflatoxin exposure, and metabolic or autonomic dysfunction[2]. A gold-standard treatment for HCC is surgery, radiation, or, sometimes, chemotherapy, depending on the stage of the cancer. There is a limited effectiveness of liver transplants, and the recurrence and survival rates are low[3]. Moreover, the clinical outcome of HCC varies according to the systemic stage, nodes, and metastases (TNM)[4], and there is no effective prognostic marker available as of yet.

Tumor aggressiveness refers to the rate at which a cancerous tumor grows and spreads to other parts of the body. Aggressiveness is an important factor in determining the prognosis and treatment options for a patient with cancer. The tumor microenvironment(TME) refers to the complex network of cellular and molecular interactions that exist within the vicinity of a tumor. It has been well established that several

factors contribute to the aggressiveness of tumors, including TME [5], yet little is known about the network that underlies this phenomenon. According to the characteristics of T cell infiltration, we stratified the patient's phenotype, prognosis and treatment choice. As part of the standard TNM staging system, monocyte, Macrophage/Monocyte and T cell regulatory cells have already been shown to have a prognostic role[6], but intrinsic features of the TME have not been studied in depth[7].

TME ecosystems are known to be greatly impacted by programmed cell death. The most common ways in which transformed hepatocytes die are apoptosis and necroptosis[8]. Necroptosis is a form of programmed cell death that is distinct from apoptosis[9]. Unlike apoptosis, which is characterized by the orderly breakdown of the cell, necroptosis is a more chaotic process in which the cell membrane becomes permeable and releases its contents into the surrounding tissue. This leads to inflammation and tissue damage. Necroptosis is activated by a variety of signals, including oxidative stress, viral infections, and exposure to certain drugs. The process is controlled by a group of proteins known as receptor-interacting proteins (RIPs), which activate an enzyme called mixed lineage kinase domain-like protein (MLKL). Then MLKL permeates the cell membrane, leading to necrosis. A variety of diseases are believed to be caused by necroptosis, including neurodegenerative diseases, cancers , and inflammatory diseases[10]. Its exact role in these diseases is not yet fully understood, and further research is required to fully understand necroptosis and its impact on health.

Necroptosis is influenced by long non-coding RNAs (lncRNAs) in various cancers, including HCC [11]. Our understanding of HCC can be improved by using lncRNA signatures to identify necroptosis and to develop new therapeutics . Further research is needed to fully understand the role of lncRNAs in HCC and the specific lncRNA signatures associated with necroptosis[12]. Nevertheless, no study has examined whether necrosis-related lncRNAs can be used to predict outcomes in HCC[13].As a solution to this problem, we discussed the effect of lymphocyte microenvironment on HCC. An analysis of lncRNA-Seq data from The Cancer Genome Atlas (TCGA) was conducted to examine the relationship between necroptosis genes and immune infiltration . TCGA data and clinical characteristics were downloaded and lncRNA data related to necroptosis was extracted. After constructing a lncRNA prognosis signature with Lasso-Cox regression analysis, the prognosis ability of the signature was tested using GEO cohorts.

MATERIALS AND METHODS

Datasets and Pre-Processing

Figure 1 illustrates the analysis flow chart .As part of the TCGA (https://portal.gdc.cancer.gov/), patients with HCC were enrolled and their lncRNA expression was assessed . We have analyzed the expression of lncRNAs in 50 normal individuals and 374 samples of tumors from the TCGA (Table 1). Taking into account previous research ,we identified 67 genes related to necrosis [14], including FADD, FAS, FASLG, MLKL, RIPK1, RIPK3, TLR3, TNF, TSC1, TRIM11, CASP8, ZBP1, MAPK8, IPMK, ITPK1, SIRT3, MYC, TNFRSF1A, TNFSF10, TNFRSF 1B, TRAF2, PANX1, OTULIN, CYLD, USP22, MAP3K7, SQSTM1, STAT3, DIABLO, DNMT1, CFLAR, BRAF AXL, ID1, CDKN2A, HSPA4, BCL2, STUB1, FLT3, HAT1, SIRT2, SIRT1, PLK1,

MPG BACH2, GATA3, MYCN, ALK, ATRX, TERT, SLC39A7, SPATA2, RNF31, IDH1, IDH2, KLF9, HDAC9, HSP90AA1, LEF1, BNIP3, CD40, BCL2L11, EGFR, DDX58, TARDBP, APP and TNFRSF21.

Differing expressions identified

According to RNA-seq (logFPKM+1 format) data, we performed Pearson correlation analysis on lncRNA and genetic markers related to necrosis (| cor |>0.15, p<0.05). Based on the TCGA cohort, a network of necroptosis-related genes as well as their prognostic values was created using the "igraph" package. Identifying genes that express differentially (DEGs) between nontumors and tumors, lncRNA from the TCGA was analyzed. Prior to comparing the expression data, we normalized the values to fragments per million (FPKM) . With the R software package "limma" the DEGs were identified.

On the basis of the expression of necroptotic regulators, Data was clustered unsupervised by consensus to identify necroptosis-related patterns for specific patients . For assessing the number and stability of clusters, the "ConsensuClusterPlus" package was used. To compare clusters, we used the limma package in R with a false discovery rate (FDR) of 0.05 and fold change absolute value >1.5 as criteria.

Functional Enrichment Analysis

For searching comprehensive information about large-scale genetic datasets, enrichment analysis was commonly used in bioinformatics. KEGG pathway enrichment analysis helped understand biological mechanisms. Our calculation was based on the gene set enrichment analysis algorithm (GSEA). GSEA (http://www.gsea-msigdb.org/gsea/index.jsp) offered statistical analysis with a 0.05 p value and 0.05 FDR . Benjamin Hochberg (BH) was applied to the p-values. A normalized enrichment score (NES) was calculated by permuting gene sets 1000 times for each analysis.

Developing and validating a prognostic model for necroptosis

According to the 1:1 ratio, 374 HCC patients were divided into training and validation sets using R . As a result of the training set analysis, the characteristics of the training set were filtered , and a model for analyzing risk was established using Minimum Absolute Selected Operator (LASSO) - Cox regression. LncRNAs related to survival were identified with a cutoff p value of 0.2 . The lncRNA's prognostic value was evaluated using Cox regression analysis. Based on univariate analysis, the Cox proportional risk model screened lncRNAs that were significantly related to the batch-adjusted survival rate (p<0.05). We constructed a LASSO regression risk model based on ten fold cross-validation in order to avoid overfitting .

Establishment and validation of the nomogram

An easy-to-use nomogram has been developed for visualizing Cox model results for clinical purposes. Prognostic factors were identified through univariate as well as multivariate Cox analyses, after that, a Cox proportional hazard model was developed. On the basis of a Cox model constructed from validation cohorts, the total points of patients were calculated. Based on median risk scores, we divided the training

queue into high and low risk groups. Following this, calibration curves and concordance indices (C indices) were calculated. Also, we performed a decision curve analysis (DCA) and plotted the time-dependent receiver operating characteristic (ROC) curve. Based on age, sex, tumor stage, and risk score, we predicted the survival rates of HCC patients after 1, 3, and 5 years .

Next, to make the model more convincing, The nomogram reliability was tested in the Gene Expression Omnibus (GEO) cohorts (https://www.ncbi.nlm.nih.gov/gds/). Similarly, by dividing the TCGA cohort's median value we were able to calculate GEO's risk scores .

Quantification of Immune Cell Infiltration

First, immune infiltration was correlated with prognosis risk signature using XCELL, EPIC, TIMER, QUANTISEQ, MCPCOUNTER, and CIBERSORT-ABS[15]. Then, to assess immune function and infiltrating cells in different subgroups, GSVA was used with the ssGSEA package in R. Finally, Using ESTIMATE, immunescores were calculated for each patient for comparison of high- and low-risk TME.

Database Expression for PD-L1

Blocking the PD-L1/PD-1 axis has demonstrated clinical benefits . Due to improved insight into the underlying regulatory mechanisms, immune checkpoint blockade has proven clinically beneficial .

Analyses of statistical data

The statistical analyses were carried out using R software (version 4.2.2) and IBM SPSS 26.0. The two-tailed $p<0.05$ resulted in significant outcome in all tests. To compare categorical variables, the chi-square test was used. To determine whether nontumor tissues and tumor tissues had similar levels of immune cell infiltration and activation, we used the Mann-Whitney U test. Prognostic signature coefficients were calculated using LASSO regression. A log-rank test was used to compare survival rates between subgroups. Using the Pearson test, we calculated the correlation. Models of Cox regression were used to assess risk factors for both univariate and multivariate analyses. The area under curves (AUCs) were calculated , and survival ROC curves were generated for 5-year OS, 3-year OS, and 1-year OS by "survival" packages. Dimensionality reduction was achieved through principal component analysis (PCA).

RESULTS

In total, 424 HCC patients were enrolled into the TCGA cohort and 95 HCC patients were enrolled into the GEO cohort. Figure 1 presents a flow chart of this study's overview. Clinical data are resumed in Table 1. The data of the study is public, so there is no need for ethical approval and informed consent.

Detection of DEGs in tumors versus non-tumors

We plotted a network using prognostic values from the TCGA cohort, along with necroptosis-related genes. The correlation network can be seen in Figure 2A, and heatmap is shown in Figure 2B. Genes

differentially expressed on the volcano plot in Figure 2C.

Signature construction for risk

A LASSO regression analysis was performed and NRLs screened to avoid overfitting (Figure 3A,B). Then, we conduct risk stratification through multiple Cox regression analysis (ENTER method) . As a follow-up, we conducted a Cox regression analysis to identify whether the risk score differed from other prognostic factors, which was shown in Figure 3C. The correlation between NRG and lncRNA can be seen in Figure 3D.

Analysis of risk groups' differential functional enrichment

We used GSEA to identify major enrichment pathways. According to the results of KEGG analysis, five most enriched pathways were selected, including cell metabolism, drug metabolism and drug sensitivity, including the metabolism of cytochrome P450 to xenobiotics, drug metabolism - cytochrome P45, retinol metabolism, bile secretion and chemical carcinogenesis - DNA adducts (Fig. 3E).

Obtaining a risk signature for validation

As shown by the Kaplan-Meier curve in the TCGA queue, there was a significant difference between the high-risk and low-risk groups regarding OS ($p < 0.001$) (Figure 4A). In the training cohorts, high-risk patients had a significantly lower OS than low-risk patients ($p < 0.001$) (Figure 4B). In the testing cohorts, OS was significantly different between high-risk and low-risk patients ($p = 0.006$) (Figure 4C). In addition, the heatmap, high-risk and low-risk group risk scores and survival status in the TCGA cohorts, the testing cohorts and the training cohorts were shown in Figure 4D,E,F, G,H,I,J,K, L.

A lncRNA-based clustering analysis of HCC patients

In order to further study, on the basis of NMF algorithm, we divided TCGA patients into subtypes. We used cluster correlation coefficient analysis, and finally decided that k=2 was the best number of nodes (Figure 5A).(Figure 5A). Applying NMF that is consistent, two clusters were defined, C1 (n = 221) and C2 (n = 122). In the PCA analysis, the two clusters were clearly distinguished from one another in their two-dimensional distribution maps (Figure 5B,5C). The result in cluster 1 was higher than that in cluster 2($p = 0.001$, Figure 5D). Furthermore, high-risk HCC patients had a lower survival rate ($p<0.001$) (Figure 5E). The correlation between cluster and risk can be seen in Figure 5F.

Construction and validation of nomograms

According to both univariate and multivariate Cox regressions in the TCGA, tumor stage and signature correlated significantly (Figures 6A ,B). Based on the K-M survival analysis, high-stage groups had a relatively worse prognosis than low-stage groups (Figures 6C,D). At 1 year, 3 year, and 5 year, the AUCs were 0.781, 0.663, and 0.686, respectively (Figure 6E), and the AUCs of risk, stage, gender, age and grade were 0.781, 0.712, 0.508, 0.492 and 0.489, respectively (Figure 6F).

According to the risk score and TNM stage, we built a nomograph to visualize the risk characteristics (Figure 7A). For 1-year, 3-year, and 5-year OS predictions, we further verified the nomogram's accuracy using the TCGA calibration curve . According to Figures 7C, based on the prediction curves, the nomogram can predict patients' overall survival quite accurately. Further, a DCA curve showed the nomogram to be highly reliable for each individual parameter (Figure 7D). Using 95 samples from the GEO cohort, we constructed a nomogram for external validation (Figure 7B).

Assessment of the immune microenvironment of Hepatocellular Carcinoma

In the two subgroups, no significant differences were observed in B cells, CD8+T cells, neutrophils, DC, T-helper cells, Th2 cells and TIL. As a result, the number of aDCs, macrophages, and Treg was significantly lower in the low-risk subgroup than in the high-risk subgroup (Figure 8A). Compared with the high-risk group, the low-risk group had a lower level of immune pathway (Figure 8B).

Using seven different calculation methods, Figure 8C illustrates the correlation between immune infiltrating cells and the associated risk characteristics .We further analyzed and found that the risk score was negatively correlated with unidentified cells, NK cells, plasmacyte-like dendritic cells, endothelial cells, hematopoietic cells, stem cells, T-cell CD8+naive, monocytes and mast cell-activated macrophages (Figure 8C). A positive correlation was also found between the risk score and uncharacterized cells, cancer-associated fibroblasts, monocytes, macrophages, and T cell regulatory (Treg) cells.

Analysis of immune checkpoints

According to our analysis of immune checkpoint expression, such as HAVCR2 , VTCN1, CD86, ICOS, CD276, LAIR1, TNFRSF9, TNFSF15 and PDCD1, there were significant differences between the low-risk and high-risk subgroups regarding immune checkpoints (Figure 9A). Moreover, the risk score correlated negatively with the expression of MIR4435−2HG, BACE1−AS, AP003390.1, AL355987.4, and NRAV , but correlated positively with PD−L1, LINC01094, AC145207.5, TMCC1−AS1, and LINC01224 (Figure 9B).

HPA database verification of PD-L1 protein expression

As shown in Figure 10 A, normal tissue and cancer tissue express PD-L1 at significantly different levels ($p < 0.001$). In Figure 10B, a significant difference was also found between high-risk and low-risk groups in TCGA when it came to PD-L1 expression ($p < 0.001$).

From the HPA dataset, immunohistochemical staining showed significant differences in the PD-L1 expression level between normal liver tissue and cancer tissue (Figure 10C; $p < 0.001$) (http://www.proteinatlas.org/) . As shown in Figure 10D, PD-L1 expression levels were higher in high-risk HCC tissues than in low-risk tissues ($p <0.001$).

DISCUSSION

Our aim was to identify a long noncoding RNA that correlates with tumor immunity microenvironment characteristics as a prognostic marker for necroptosis in HCC. We obtained clinical data and lncRNA expression profiles from the TCGA database. Multivariate Cox analysis, univariate Cox analysis, and LASSO analysis were applied to determine the necrosis-related genes in two steps. By combining differentially expressed lncRNA signatures related to necroptosis, prognosis was predicted. High-predictability nomogram was developed by combining the necroptosis-related lncRNAs signature with clinical characteristics. In this study, using the TCGA cohorts involving 374 HCC patients, we performed a comprehensive model of the lncRNA involved in the necroptotic pathway, and tested our preliminary hypothesis using 95 HCC patients from the GEO cohorts.

The findings suggest that there may be a relationship between certain immune cell populations, such as aDCs, macrophages, and Treg cells, and the risk of disease. Specifically, lower levels of these immune cells were found in the low-risk subgroup, while higher levels of uncharacterized cells, cancer associated fibroblasts, monocytes, macrophages/monocytes, and Treg cells were found in the high-risk subgroup. The positive correlation between the risk score and these immune cell populations suggests that they may play a role in determining disease risk. A correlation was found between PD-L1 expression and necroptosis-related lncRNAs in HCC tissues. These relationships requireed further research to be fully understood. The present study found significantly higher levels of PD-L1 in HCC tissues in patients in high-risk groups compared to those in low-risk groups, indicating high-risk patients may develop HCC.

The tumor microenvironment encompasses a range of different cell types, including cancer cells, immune cells, blood vessels, fibroblasts, and extracellular matrix components. These interactions play a crucial role in shaping the behavior and progression of tumors, both by promoting tumor growth and by regulating the immune response to the cancer cells. Studies have shown that the tumor microenvironment has an influence on the development and spread of cancer, including tumor angiogenesis, invasion and immune escape. Understanding the complex interactions within the tumor microenvironment is an important area of research, as it can provide new insights into cancer diagnosis and treatment .

Researchers previously reported that long coding RNAs play a role in the immune evasion of HCC [16]. In line with this, the results of this study showed that there was a significant difference between high-risk tumors and low-risk tumors. The immune characteristics were activated with the increase of risk score, and the proportion of Tregs increased accordingly. In view of these data, we believed Tregs may contribute to the microenvironment of HCC tumors [17], and immunotherapy may be beneficial for patients with a low risk score .

Immune checkpoint molecules are proteins that regulate the immune system's response to foreign invaders such as cancer cells. These molecules act as "checkpoints" that determine whether the immune system should attack a particular target. In normal circumstances, immune checkpoint molecules prevent the immune system from attacking healthy cells and tissues, but some cancers can take advantage of these checkpoints to evade the immune system's response.

Targeting immune checkpoint molecules has emerged as a promising strategy for cancer therapy. By blocking the activity of these checkpoints, researchers aim to restore the immune system's ability to detect and attack cancer cells. Some of the most well-known immune checkpoint molecules include CTLA-4, PD-1, and PD-L1. Drugs that target these checkpoints, such as ipilimumab, nivolumab, and pembrolizumab, have been approved for the treatment of several types of cancer, including melanoma, lung cancer, and renal cell carcinoma.

Through immune editing, tumor cells can avoid immune recognition[18]. PD-L1 (programmed cell death ligand 1) is an immune checkpoint molecule that can be modified during immunity editing[19]. The interaction between PD-1 and PD-L1, found on tumor cells, prevents the immune system from destroying cancer cells by activating and expanding T cells [20]. PD-L1/PD-1 immune checkpoint blockades have shown clinical benefits[21]. Since the tumor microenvironment is immunosuppressive, these treatments are not effective for most patients [22]. As a consequence, anti-PD-1/PD-L1 treatments must improve their efficacy by understanding the molecular mechanisms underlying PD-L1 regulation [23] .

There were limitations to this study .First of all, our research on the data extracted from the TCGA database belonged to retrospective analysis[24]. In addition, using gene knockout hepatoma models, we will study the effects of lncRNAs associated with necroptosis on tumor progression and immunotherapy efficacy [25]. Multiple centers should be involved in large-scale, prospective research in the future .

Conclusions

Therefore, we conclude that lncRNA has immunogenetic properties in human HCC. Considering these factors, it is very important for us to conduct more research in the future to better evaluate their composition, function and evolutionary characteristics, as well as possible checkpoints for the immune environment related to the characteristics of necrosis, so as to explore new therapeutic possibilities.

Declarations

Acknowledgements

We are very grateful for the platform provided by TCGA database and GEO database, as well as the contributors who provided meaningful data sets.

Material and data availability

In this study, the datasets generated are available in the TCGA (https:// portal.gdc.cancer.gov), the Gene Expression Omnibus (https:// www.ncbi.nlm.nih.gov) and HPA (https://www.proteinatlas.org).

The link to the database where the data can be accessed is in the [jianguoyun]repository, (https://www.jianguoyun.com/c/sd/15c2f53/320121052627aa5b).

Approval of ethics and consent to participate

Neither the authors nor any of the participants in this article have conducted studies with humans or animals .

Interests competing with each other

It is declared that the authors have no conflict of interest.

References

1. Chunxue Yang, Derek Lee, Misty Shuo Zhang, Aki Pui-Wah Tse, Lai Wei, Macus Hao-Ran Bao, Bowie Po-Yee Wong, Cerise Yuen-Ki Chan, Vincent Wai-Hin Yuen, Yiling Chen, and Carmen Chak-Lui Wong*. Genome-Wide CRISPR/Cas9 Library Screening Revealed Dietary Restriction of Glutamine in Combination with Inhibition of Pyruvate Metabolism as Effective Liver Cancer Treatment. Advanced Science, 2022, 9, 2202104, 1-15 doi: 1002/advs.202202104
2. Katrin Böttcher, Massimo Pinzani .Pathophysiology of liver fibrosis and the methodological barriers to the development of anti-fibrogenic agents. Adv Drug Deliv Rev. 2017 Nov 1;121:3-8.doi: 10.1016/j.addr.2017.05.016. Epub 2017 Jun 9.
3. Chris Estes, Homie Razavi , Rohit Loomba , Zobair Younossi , Arun J Sanyal .Modeling the epidemic of nonalcoholic fatty liver disease demonstrates an exponential increase in burden of disease. Hepatology. 2018 Jan;67(1):123-133. doi: 10.1002/hep.29466. Epub 2017 Dec 1.\
4. Xiulei Zhang, Zhihao Fu, and Xiao Zhang.TP53 Mutation Related and Directly Regulated lncRNA Prognosis Markers in Hepatocellular Carcinoma. Onco Targets Ther.2021; 14: 4427–4437.doi: 2147/OTT.S321669
5. Lihong Wang, Louisa S Chard Dunmall, Zhenguo Cheng, and Yaohe Wang. Remodeling the tumor microenvironment by oncolytic viruses: beyond oncolysis of tumor cells for cancer treatment. J Immunother Cancer. 2022; 10(5): e004167.doi: 10.1136/jitc-2021-004167
6. Emily Cassar, Apriliana E. R. Kartikasari,and Magdalena Plebanski. Regulatory T Cells in Ovarian Carcinogenesis and Future Therapeutic Opportunities. Cancers (Basel). 2022 Nov; 14(22): 5488. doi: 10.3390/cancers14225488
7. Yuan Qin, Wei Sun, Zhihong Wang,Wenwu Dong,Liang He,Ting Zhang,and Hao Zhang. Long Non-Coding Small Nucleolar RNA Host Genes (SNHGs) in Endocrine-Related Cancers. Onco Targets Ther. 2020; 13: 7699–7717.doi: 10.2147/OTT.S267140
8. Behrouz Hassannia , Peter Vandenabeele , Tom Vanden Berghe . Targeting Ferroptosis to Iron Out Cancer. Cancer Cell. 2019, 10;35(6):830-849. doi: 10.1016/j.ccell.2019.04.002.
9. Damien Bertheloot, Eicke Latz, and Bernardo S. Franklin. Necroptosis, pyroptosis and apoptosis: an intricate game of cell death. Cell Mol Immunol. 2021, 18(5): 1106–1121.
10. Sofie Martens Jolien Bridelance,Ria Roelandt,Peter Vandenabeele,and Nozomi Takahashi. MLKL in cancer: more than a necroptosis regulator. Cell Death Differ. 2021 Jun; 28(6): 1757–1772.doi: 10.1038/s41418-021-00785-0

11. Yun Ma, Guijie Guo, Tingting Li, Faxin Wen, Jianling Yang, Biao Chen, Xuefei Wang, and Ji-Long Chen. A novel imatinib-upregulated long noncoding RNA plays a critical role in inhibition of tumor growth induced by Abl oncogenes. Mol Cancer. 2022; 21: 5. doi: 10.1186/s12943-021-01478-5
12. Shan Lu, Jiansheng Zhou,Yimin Sun, Nan Li, Mingyong Miao,Binghua Jiao,and Huan Chen. The noncoding RNA HOXD-AS1 is a critical regulator of the metastasis and apoptosis phenotype in human hepatocellular carcinoma. Mol Cancer. 2017; 16: 125. doi: 10.1186/s12943-017-0676-x
13. Yuanyuan Wu,Liwen Hu,Yan Liang,Juan Li, Kai Wang,Xuedan Chen, Hui Meng, Xingying Guan,Kang Yang, and Yun Bai. Up-regulation of lncRNA CASC9 promotes esophageal squamous cell carcinoma growth by negatively regulating PDCD4 expression through EZH2. Mol Cancer. 2017; 16: 150.doi: 10.1186/s12943-017-0715-7
14. Aibin Liu,Yanyan Li, Lin Shen, Na Li, Liangfang Shen, and Zhanzhan Li. Pan-cancer analysis of a novel indicator of necroptosis with its application in human cancer . Aging (Albany NY). 2022 Sep 29; 14(18): 7587–7616.doi: 10.18632/aging.204307
15. Lei Peng, Jingbin Ji, Chenyu Zhang, Zhe Wu, Yuhui Sun, Kun Fan, Wenxing Du, Ao Liu, and Wenjie Jiao. Development and validation of a prognostic risk signature for lung adenocarcinoma constructed by six ferroptosis, necroptosis, and pyroptosis-related lncRNAs. J Thorac Dis. 2022 Oct; 14(10): 3955–3974.doi: 10.21037/jtd-22-1151
16. Shiuli Agarwal,Tim Vierbuchen,Sreya Ghosh,Jennie Chan,Zhaozhao Jiang,Richard K. Kandasamy,Emiliano Ricci,and Katherine A. Fitzgerald. The long non-coding RNA LUCAT1 is a negative feedback regulator of interferon responses in humans. Nat Commun. 2020; 11: 6348.doi: 10.1038/s41467-020-20165-5
17. Jing Wang , Yanzhou Chang , Hui Luo, Wenxiao Jiang , Ligeng Xu , Tianfeng Chen , Xueqiong Zhu . Designing immunogenic nanotherapeutics for photothermal-triggered immunotherapy involving reprogramming immunosuppression and activating systemic antitumor responses. Biomaterials. 2020 Oct;255:120153. doi: 10.1016/j.biomaterials.2020.120153.
18. Ju Yeon Lee,Hyun Tae Lee,Woori Shin,Jongseok Chae,Jaemo Choi,Sung Hyun Kim,Heejin Lim,Tae Won Heo,Kyeong Young Park,Yeon Ji Lee,Seong Eon Ryu,Ji Young Son,1 Jee Un Lee,and Yong-Seok Heoa. Structural basis of checkpoint blockade by monoclonal antibodies in cancer immunotherapy. Nat Commun. 2016; 7: 13354. doi: 10.1038/ncomms13354
19. Ramon Arens , Ferenc A Scheeren . Genetic Screening for Novel Regulators of Immune Checkpoint Molecules. Trends Immunol. 2020 Aug;41(8):692-705. doi: 10.1016/j.it.2020.06.005.
20. Ching-Chieh Weng,Mei-Jen Hsieh,Chia-Chen Wu, Yu-Chun Lin,Yan-Shen Shan,Wen-Chun Hung,Li-Tzong Chen,and Kuang-Hung Cheng. Loss of the transcriptional repressor TGIF1 results in enhanced Kras-driven development of pancreatic cancer. Mol Cancer. 2019; 18: 96.doi: 10.1186/s12943-019-1023-1
21. Yimeng Ren,Yun Qian,Luoyan Ai,Yile Xie,Yaqi Gao,Ziyan Zhuang,Jinxian Chen,Ying-Xuan Chen,and Jing-Yuan Fang. TRAPPC4 regulates the intracellular trafficking of PD-L1 and antitumor immunity. Nat Commun. 2021; 12: 5405.doi: 10.1038/s41467-021-25662-9

22. Krupa Naran, Trishana Nundalall, Shivan Chetty, Stefan Barth. Principles of Immunotherapy: Implications for Treatment Strategies in Cancer and Infectious Diseases .Front Microbiol . 2018 Dec 21;9:3158. doi: 10.3389/fmicb.2018.03158.
23. Hui Li, Xinwei Kuang, Long Liang, Youqiong Ye, YongChang Zhang, Jialu Li, Fangyu Ma, Juan Tao, Guang Lei, Shuang Zhao, Juan Su, Nong Yang, Cong Peng, Xiaowei Xu, Mien-Chie Hung, Leng Han, Hong Liu, Jing Liu,and Xiang Chen. The Beneficial Role of Sunitinib in Tumor Immune Surveillance by Regulating Tumor PD-L1. Adv Sci (Weinh). 2021 Jan; 8(2): 2001596. doi: 10.1002/advs.202001596
24. Hunain Alam, Ming Tang, Mayinuer Maitituoheti,Shilpa S. Dhar,Manish Kumar,Chae Young Han, Chandra Shekar R Ambati,Samir B. Amin,Bingnan Gu,Tsai-Yu Chen,Yu-Hsi Lin,Jichao Chen,Florian L. Muller,Nagireddy Putluri,Elsa R. Flores,Francesco J. DeMayo, Laura Baseler,Kunal Rai,and Min Gyu Lee. KMT2D deficiency impairs super-enhancers to confer a glycolytic vulnerability in lung cancer. Cancer Cell. 2020 Apr 13; 37(4): 599-617.e7.doi: 10.1016/j.ccell.2020.03.005
25. Yuta Myojin , Hayato Hikita , Masaya Sugiyama , Yoichi Sasaki , Kenji Fukumoto , Sadatsugu Sakane , Yuki Makino , Nobuyuki Takemura , Ryoko Yamada , Minoru Shigekawa , Takahiro Kodama , Ryotaro Sakamori , Shogo Kobayashi , Tomohide Tatsumi , Hiroshi Suemizu , Hidetoshi Eguchi , Norihiro Kokudo , Masashi Mizokami , Tetsuo Takehara . Hepatic Stellate Cells in Hepatocellular Carcinoma Promote Tumor Growth Via Growth Differentiation Factor 15 Production. Gastroenterology. 2021 Apr;160(5):1741-1754.e16. doi: 10.1053/j.gastro.2020.12.015. Epub 2020 Dec 17.

Tables

TABLE 1 Clinical features of TCGA

Variables	Count	Percentage (%)
Age (mean±SD)	59.45 ±13.34	
Status		
Alive	267	63.88
Dead	151	36.12
Gender		
Male	272	65.07
Female	146	34.93
Pathological stage		
Stage I	194	46.41
Stage II	98	23.44
Stage III	7	1.67
Stage IIIA	65	15.55
Stage IIIB	9	2.15
Stage IIIC	9	2.15
Stage IV	3	0.72
Stage IVA	4	0.96
Stage IVB	5	1.2
Unknown	24	5.74
T staging		
T1	204	48.80
T2	98	23.44
T2a	5	1.2
T2b	4	0.96
T3	54	12.92
T3a	29	6.94
T3b	7	1.67
T4	14	3.35
TX	1	0.24

Unknown	2	0.48
M staging		
M0	303	72.49
M1	8	1.91
MX	107	25.60
N staging		
N0	290	69.38
N1	8	1.91
NX	119	28.47
Unknown	1	0.24
Grade		
G1	55	13.16
G2	180	43.06
G3	124	29.67
G4	13	3.11
Unknown	46	11.00

Figures

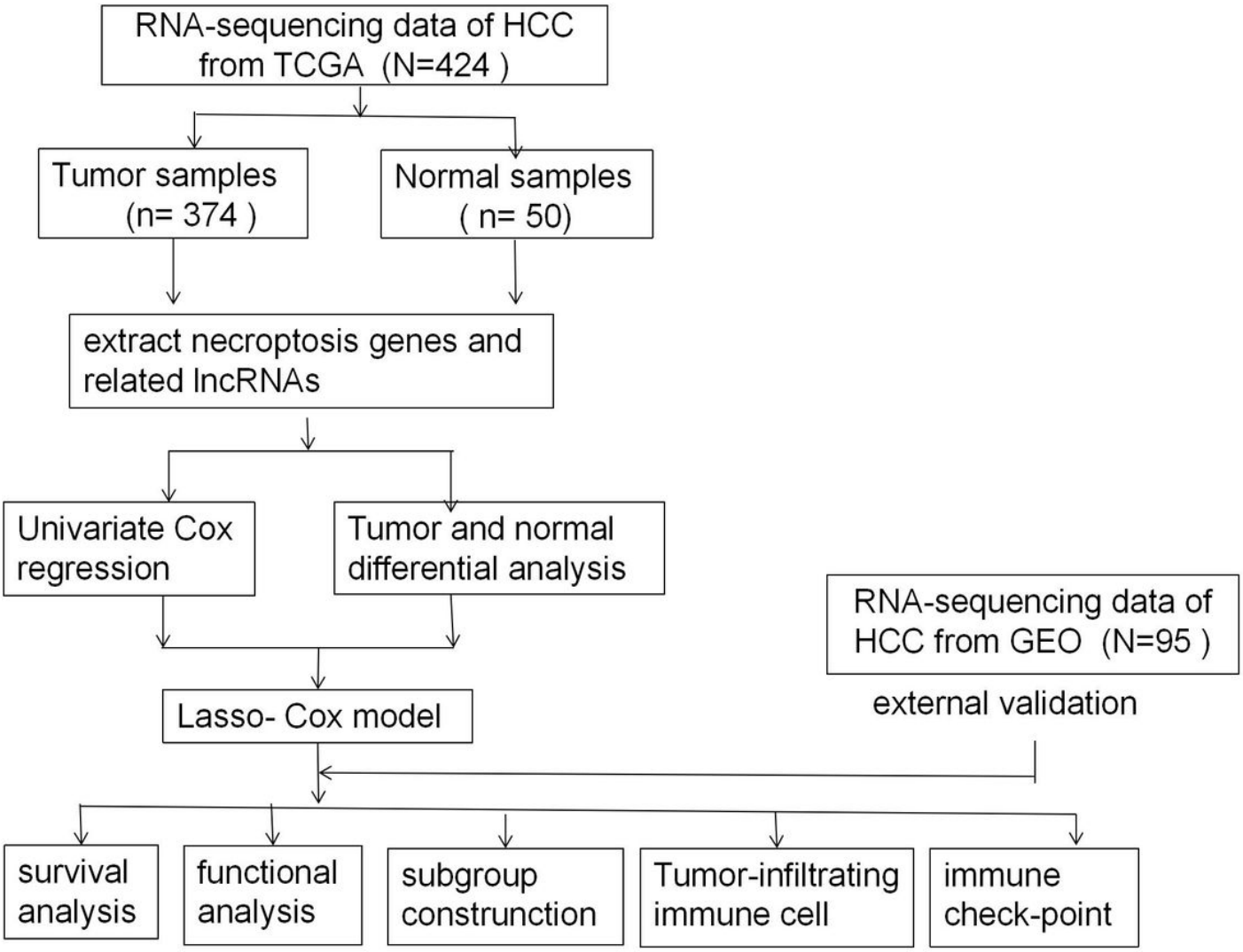

Figure 1

Study's roadmap

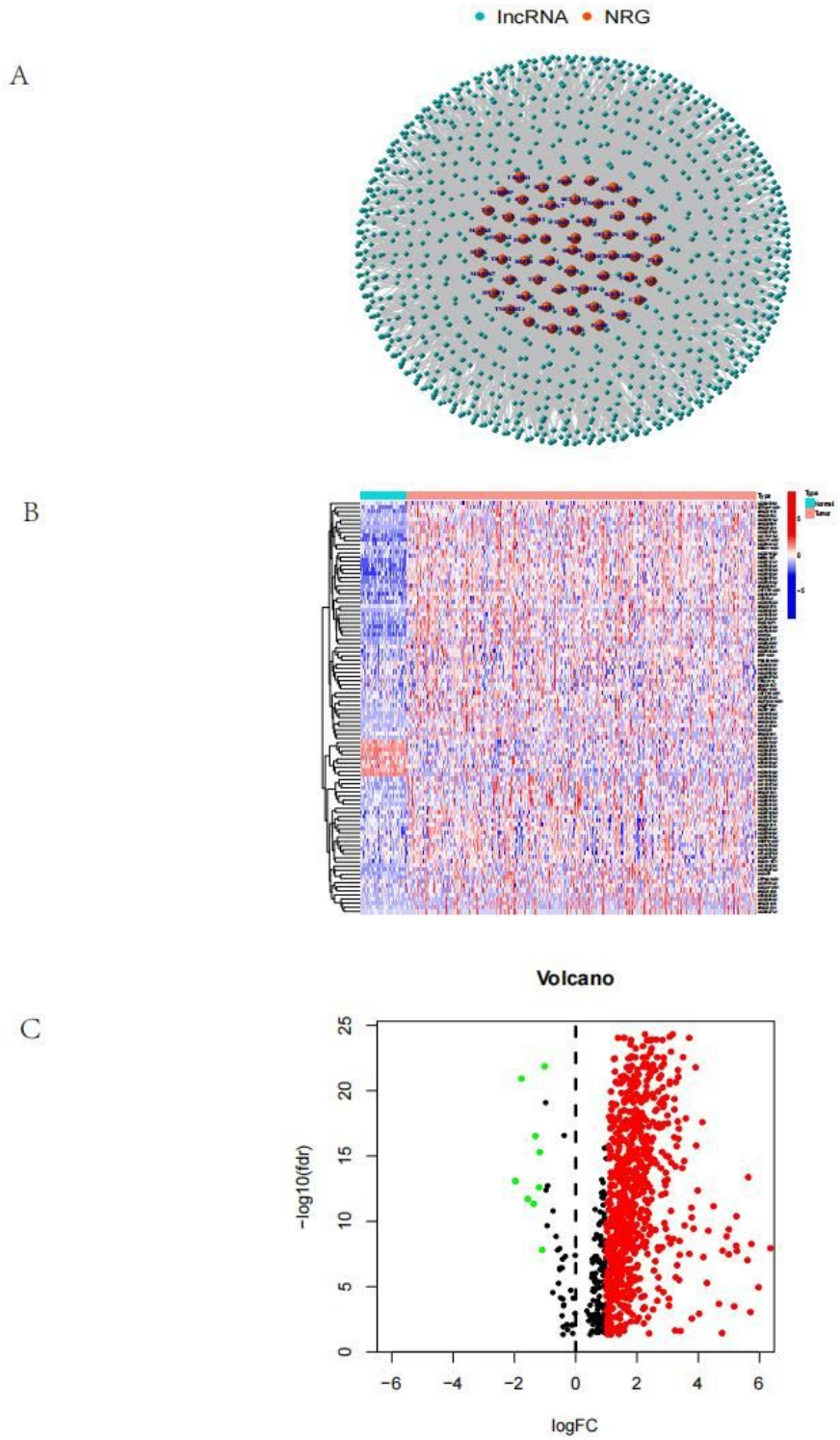

Figure 2

Identification of lncRNAs:

(A) The correlation network

(B) heatmap

(C) Volcano map

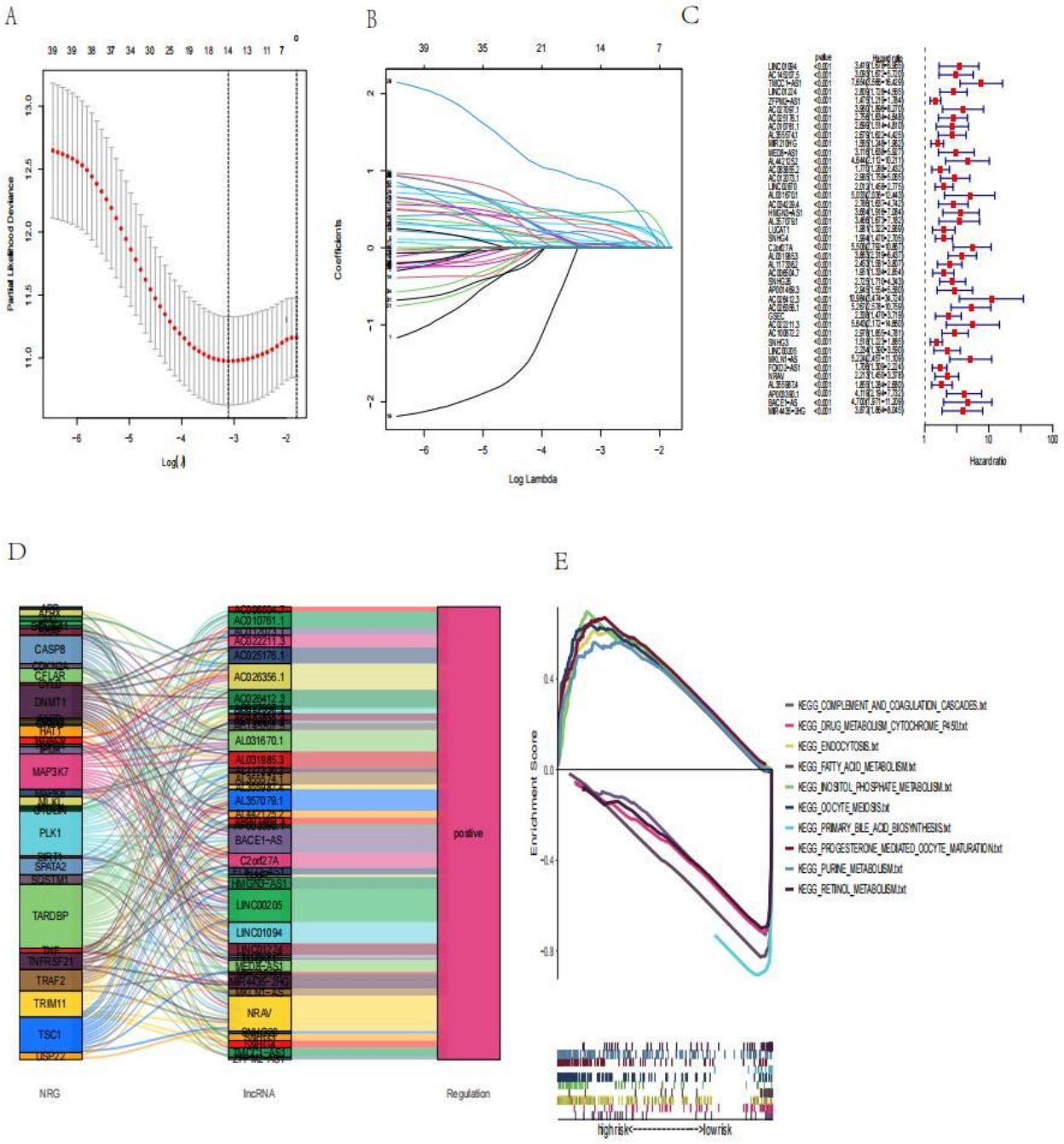

Figure 3

Construction of the lncRNA signature:

(A) LASSO was used in the 10-fold cross-validation.

(B) Optimized lambda coefficient profiles for LASSO

(C) Plot of forest for univariate results

(D) Sankey diagram depicting the associations between NRG and lncRNA

(E) GSEA of the first five routes

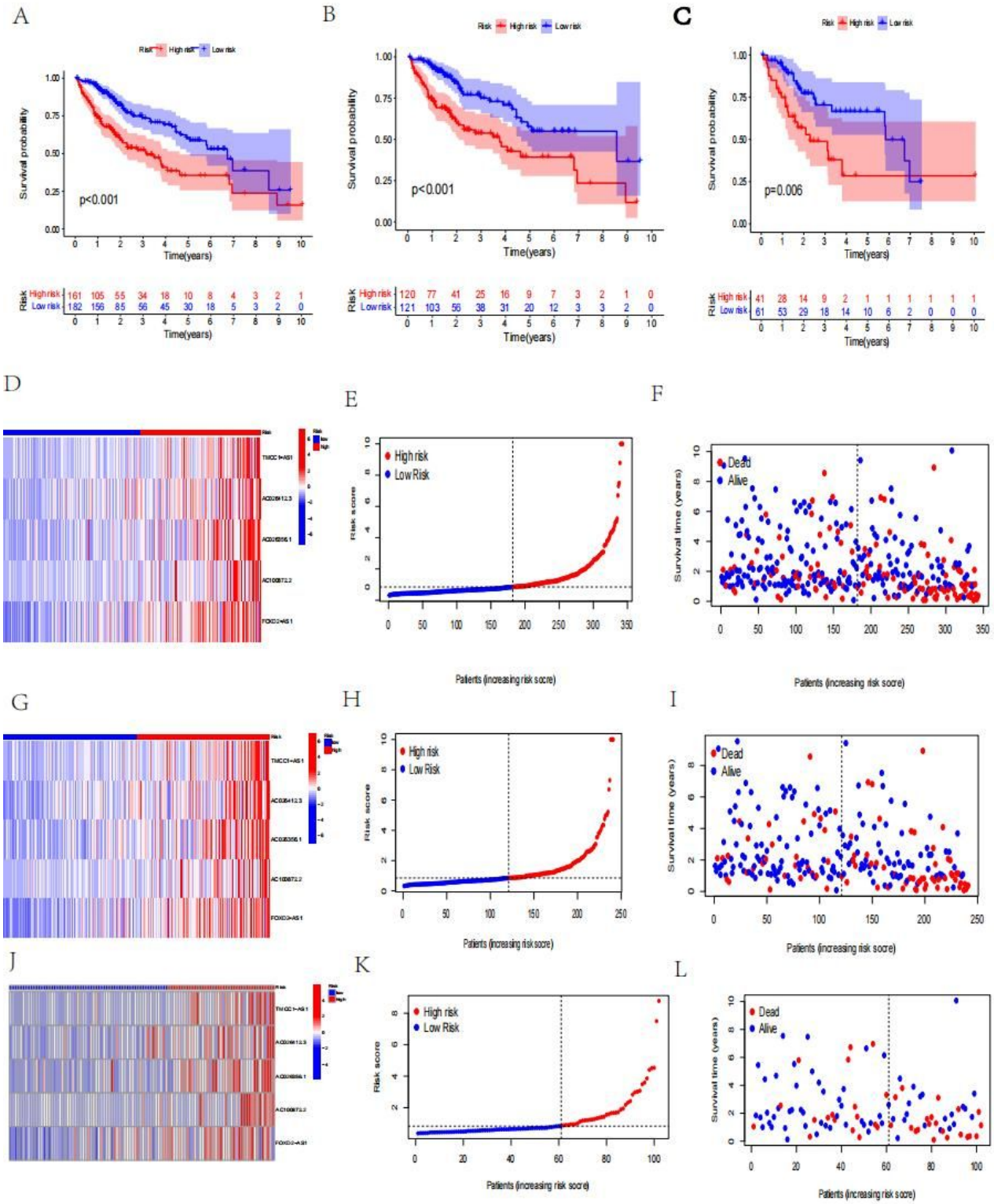

Figure 4

TCGA prognostic signature evaluation

(A) TCGA OS curves showing high versus low risk

(B) OS curves showing the association between high and low risk in training

(C) OS curves showing the association between high and low risk in testing

(D) A heatmap from the TCGA

(E)Risk score distribution

(F) TCGA OS status

(G) Heatmap in the training set

(H) Risk scores for training sets

(I) Training set OS status

(J) Heatmap in the testing set

(K) Risk scores for testing sets

(L) testing set OS status

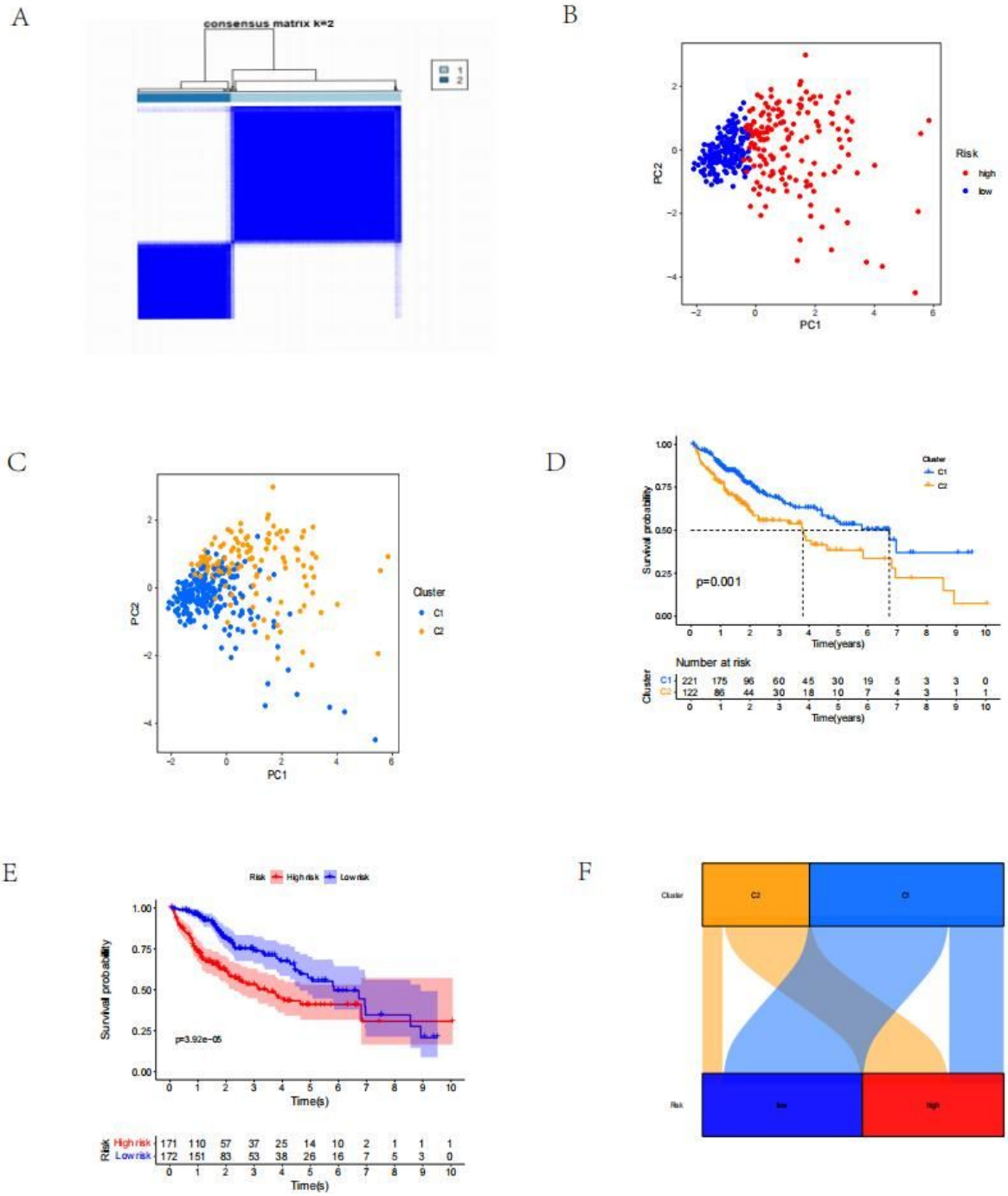

Figure 5

Different subtypes identifified by risk signature

(A) Using the clustering algorithm, the TCGA was divided into two clusters

(B) A risk PCA

(C) Cluster PCA

(D) Observations on OS in two clusters based on Kaplan-Meier survival curves

(E) Survival curves for high and low risk groups according to Kaplan-Meier

(F) Sankey diagram depicting the associations between cluster and risk

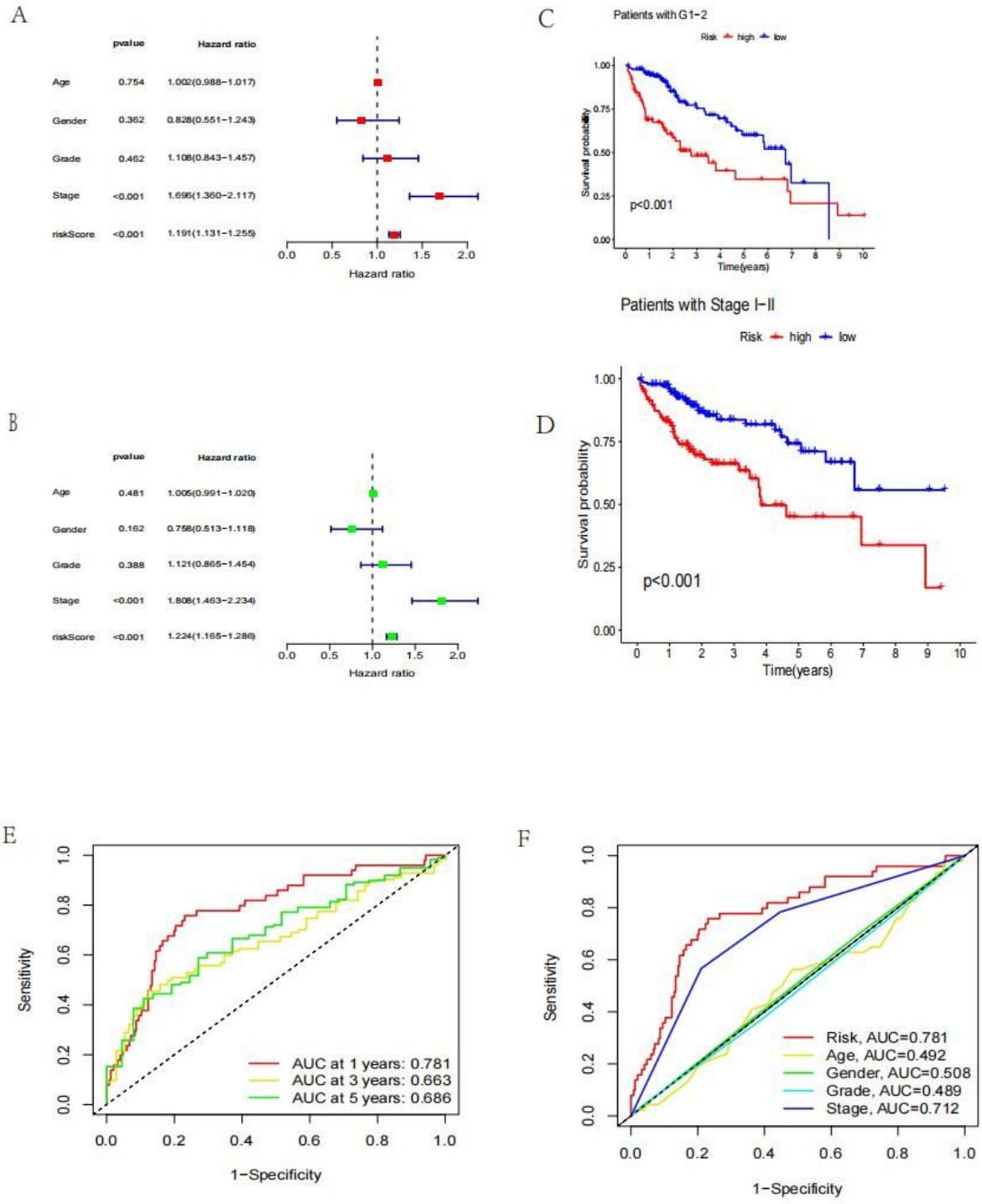

Figure 6

Evaluation of prognostic characteristics

(A) Univariate analysis of TCGA

(B) Multivariate analysis of TCGA

(C) Comparison of survival rates in groups of high grades and low grades using the Kaplan-Meier method

(D) Comparison of survival rates in groups of high grades and low stage using the Kaplan-Meier method

(E) ROC curve in TCGA queue. 1. The AUC of OS in 3 and 5 years is 0.781, 0.663 and 0.686 respectively

(F) ROC curve in TCGA queue. The AUC of risk, stage, gender, age and grade are 0.781, 0.712, 0.508, 0.492 and 0.489 respectively

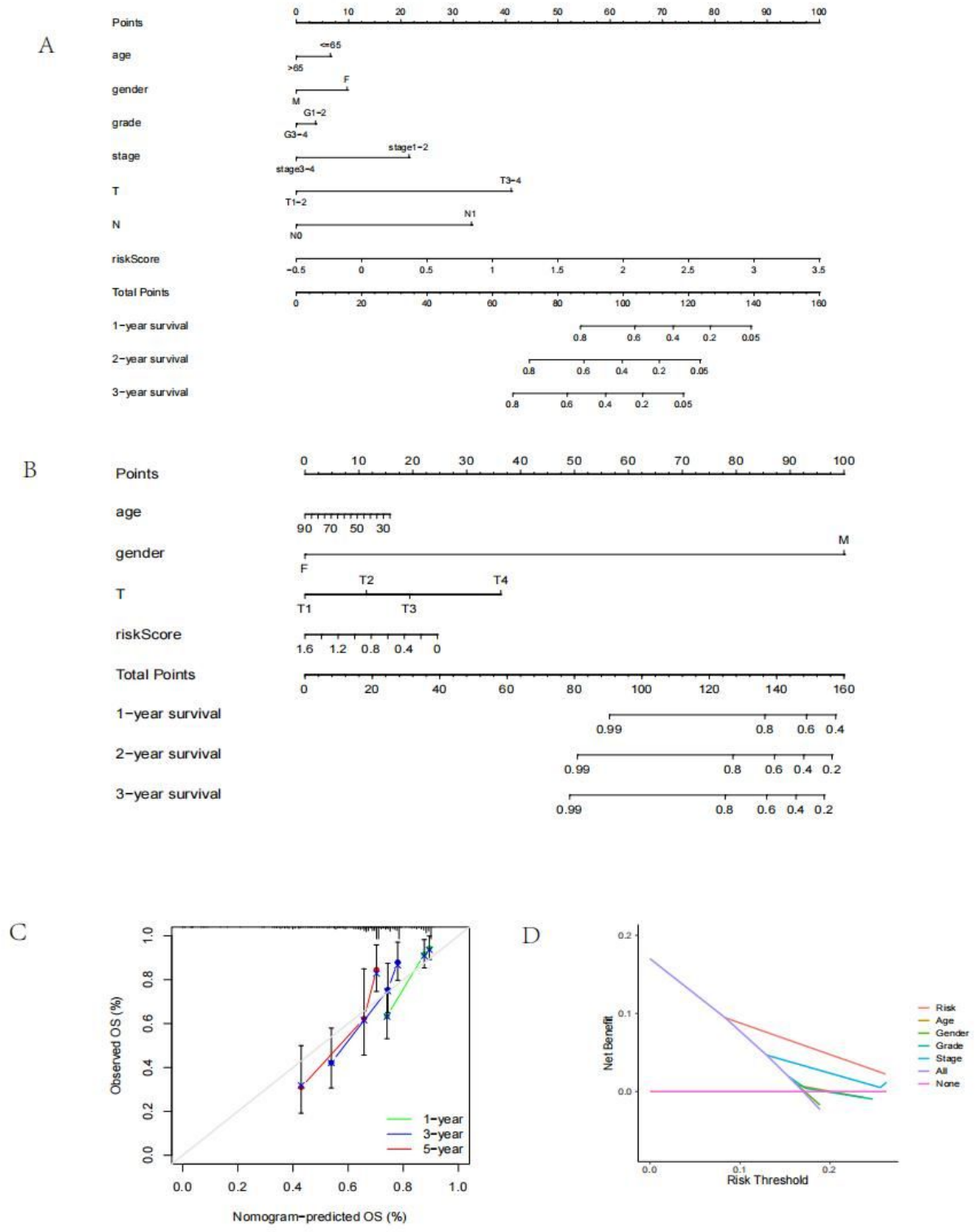

Figure 7

Prediction of OS using nomograms

(A) Clinical and OS signature nomograms for HCC in the TCGA

(B) Clinical and OS signature nomograms for HCC in the GEO

(C) Nomogram calibration curve for assessing OS prediction reliability

(D) DCA curve showing the signature's clinical utility

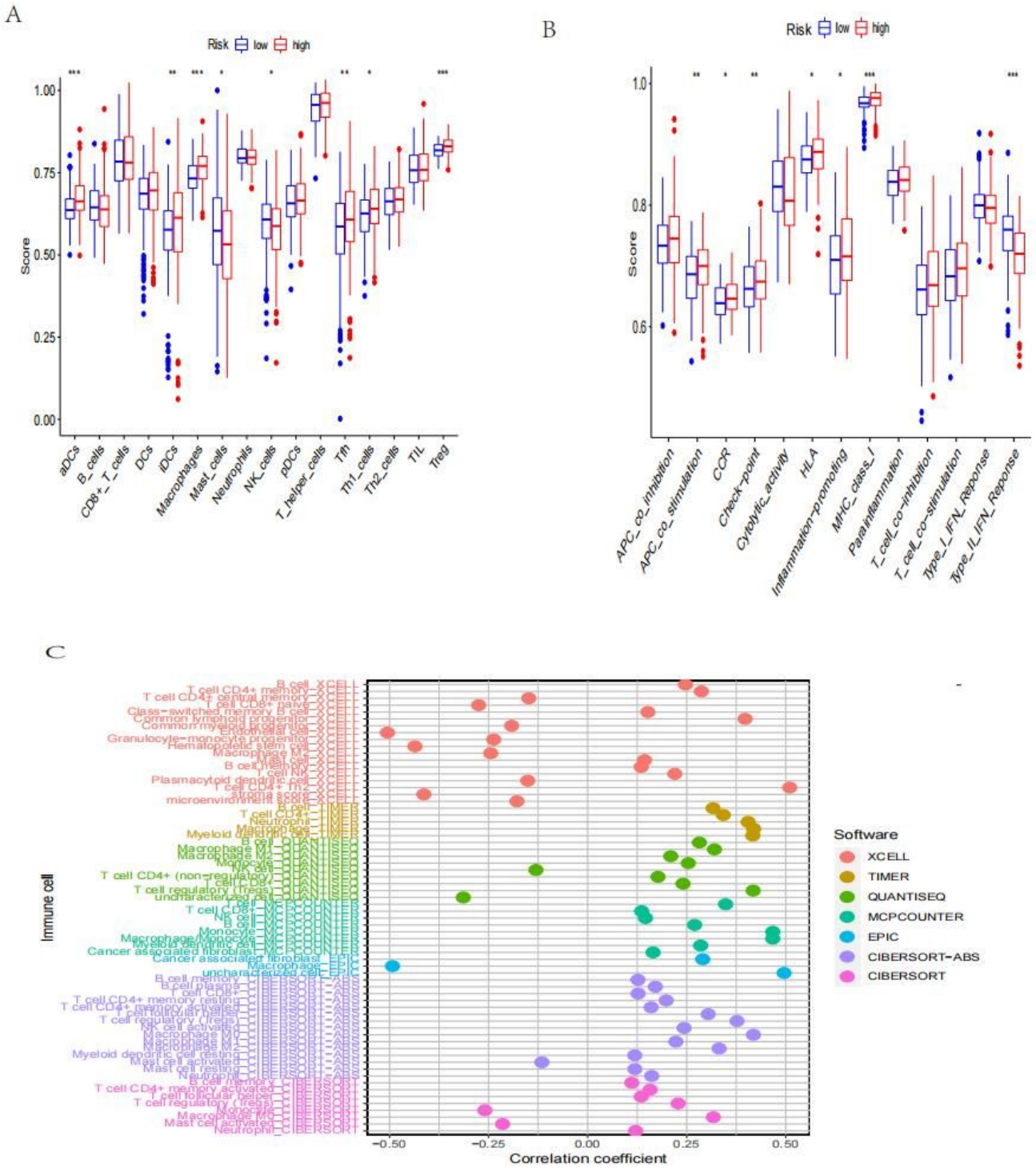

Figure 8

Evaluation of tumor immune microenvironment

(A) Immunocyte box diagram

(B) Block diagram of biological pathways

(C) Heat map of immune cell infiltration based on CIBERSORT, CIBERSORT-ABS, QUANTISEQ, XCELL, MCPCOUNTER, EPIC and TIMER algorithms

* p<0.05 ** p<0.01 *** p<0.001

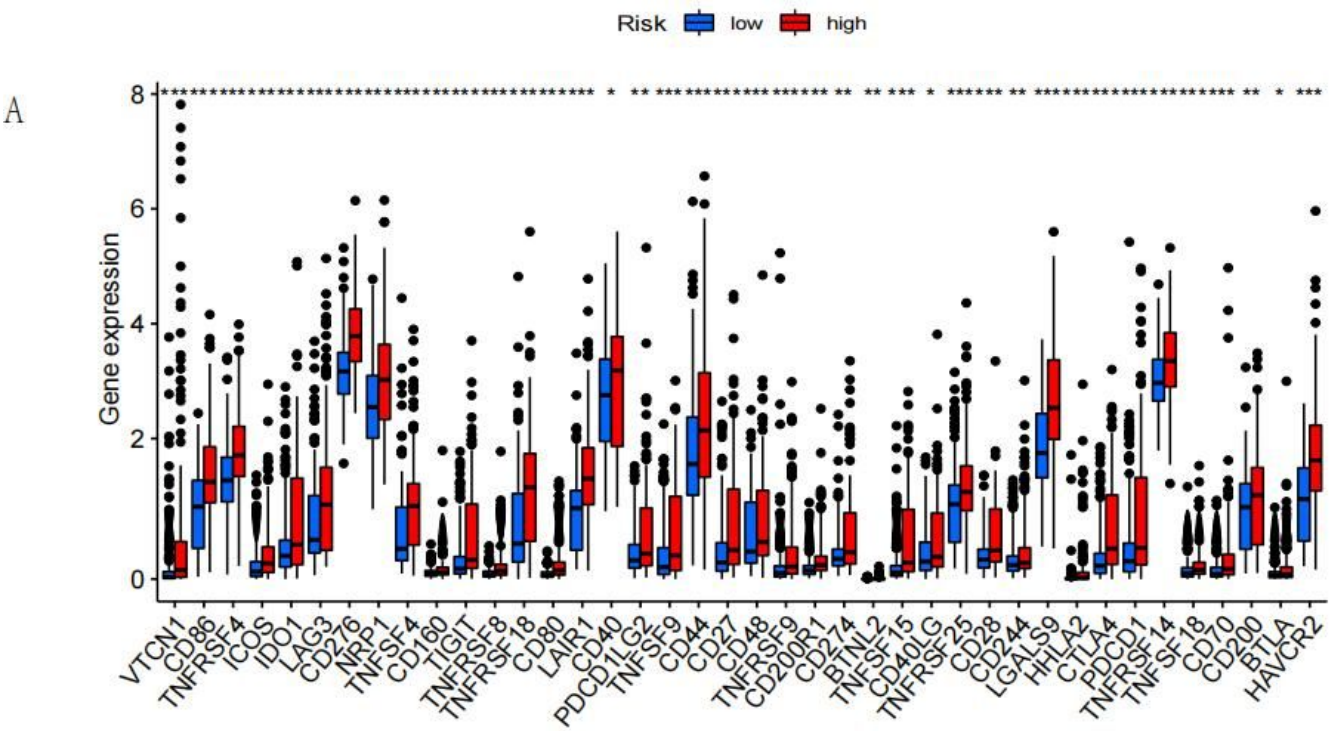

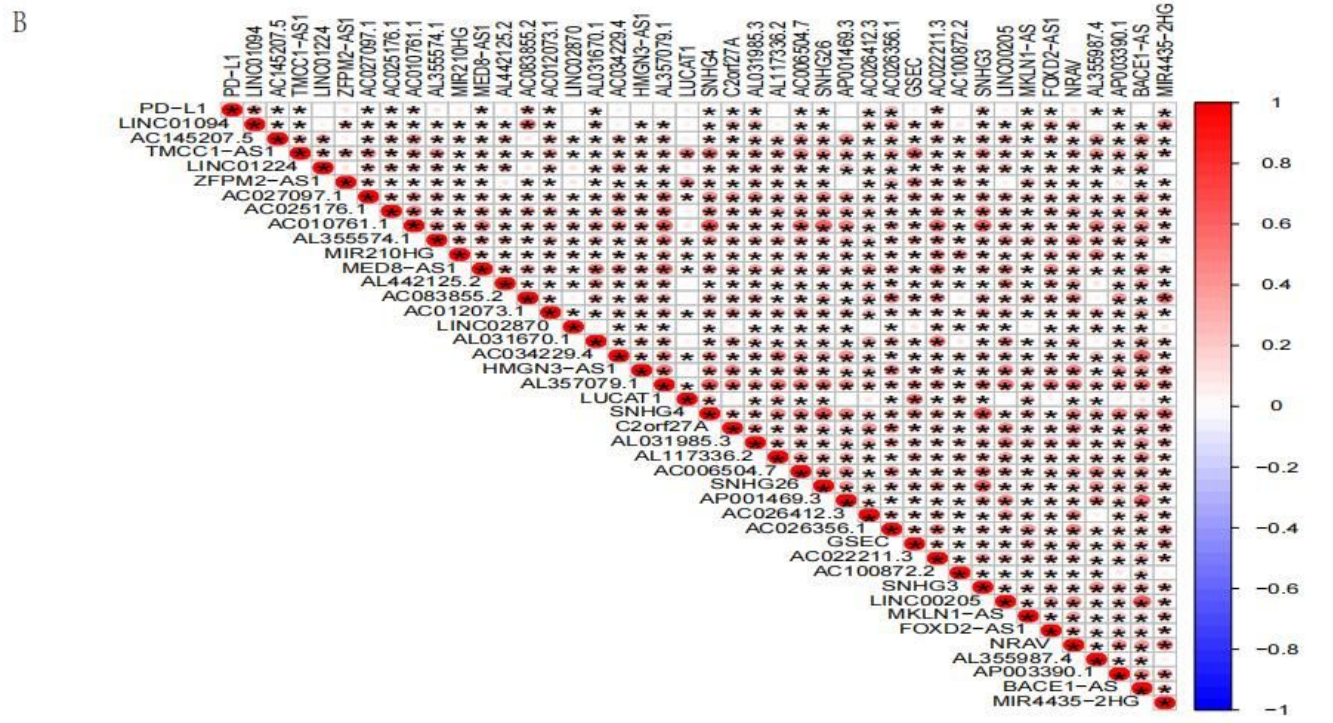

Figure 9

Analysis of immune checkpoints

(A) Expression of immune checkpoint between two subgroups

(B) correlation analysis among immune checkpoints

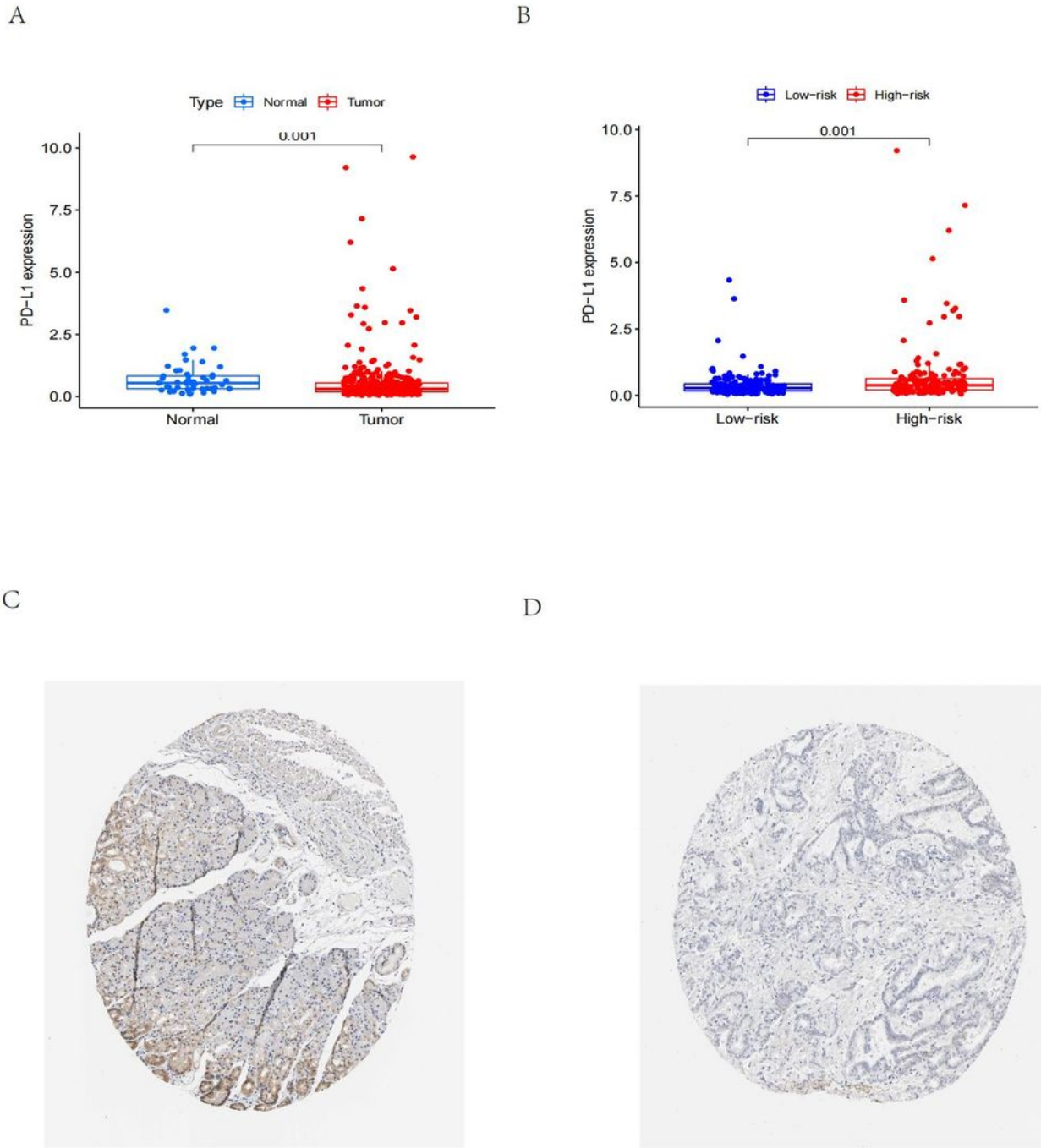

Figure 10

PD-L1 protein expression

(A) PD−L1 expression between Normal and Tumor

(B) PD−L1 expression between high-risk and low-risk group

(C) Normal tissues derived from the HPA database

(D) Tumor tissues derived from the HPA database